CHEMISTRY
A EUROPEAN JOURNAL

DOI: 10.1002/chem.200800875

# Reactions of Uranium Atoms with Ammonia: Infrared Spectra and Quasi-Relativistic Calculations of the U:$NH_3$, $H_2N{-}UH$, and $HN{=}UH_2$ Complexes

**Xuefeng Wang,[a] Lester Andrews,*[a] and Colin J. Marsden[b]**

**Abstract:** Ammonia molecules interact with U atoms, and the resulting U:$NH_3$ complex rearranges upon visible irradiation to form the $H_2N{-}UH$ and $HN{=}UH_2$ molecules in excess argon. These products are identified by functional group frequencies, $^{15}NH_3$ and $ND_3$ isotopic shifts, and comparison to frequencies calculated by using density functional theory. The N=U π bond in $HN{=}UH_2$ is enhanced by partial triple-bond character through N(2p) to U(5f) conjugation, which is comparable to that found in the analogous $HN{=}ThH_2$ molecule. These products also form complexes with additional ammonia molecules in the matrix. The interesting higher-energy $N{\equiv}UH_3$ complex is not formed.

**Keywords:** density functional calculations · IR spectroscopy · matrix isolation · uranimine · uranium

## Introduction

Several imido analogues of the uranyl dication ($UO_2^{2+}$) have recently been synthesized. These R−N=U=N−R compounds contain short ((1.85 ± 0.01) Å) multiple bonds to uranium.[1] The simple NUN molecule, which is isoelectronic to uranyl, has been characterized experimentally only by matrix isolation spectroscopy, and a 1.73 Å bond length has been computed by using the B3LYP density functional.[2–4] A comparable short 1.74 Å N≡U triple bond has been predicted for NUIr.[5] A molecular actinide complex containing a metal–nitride unit has been synthesized, which opens the way to new comparative investigations of metal–ligand multiple bonds.[6] The simple terminal uranium nitride complex $N{\equiv}UF_3$ has recently been prepared in this laboratory from the favorable reaction of U atoms and $NF_3$ molecules.[7] The $N{\equiv}UF_3$ molecule contains a strong uranium nitrogen triple bond with calculated 1.76 (CASPT2) and 1.75 Å (PW91) lengths. Important chemical applications of multiple bonds with actinide elements have been discussed.[8]

Recently, thorimine, $HN{=}ThH_2$, has been investigated in our laboratories, and the role of 5f orbitals in the formation of additional π bonding through conjugation of the nitrogen lone electron pair has been addressed.[9] How will $HN{=}UH_2$ with electrons already in 5f orbitals behave toward the formation of additional N−U π bonding? Thorimine, $HN{=}ThH_2$, and the Group 4 analogues are structurally quite different from the simplest organic imine, methyleneimine,[10–13] and conjugation of the nitrogen lone pair to the metal center plays a vital role in the bonding and structure of these metal imine molecules. The role of Th 5f orbital radial overlap in methane activation has been highlighted.[14] In the comparison with uranium, the known stability of the $U^{VI}$ state invites consideration of the possible interesting $N{\equiv}UH_3$ molecule, since the analogous Group 6 molecules $N{\equiv}MoH_3$ and $N{\equiv}WH_3$ have just been prepared in this laboratory.[15]

The related methylidene molecules $CH_2{=}ThH_2$ and $CH_2{=}UH_2$ have been formed by methane activation through reaction of the laser-ablated actinide metal atoms, and calculations have shown that the uranium species has a shorter double bond and more agostic distortion.[16–18] Such distortion has been discussed in the analogous early transition-metal complexes, where in contrast it decreases in the Group 4 to 5 to 6 methylidene complex series.[18,19]

We report here the first experimental and theoretical evidence for the simple uranimine, $HN{=}UH_2$, and explore the multiple bonding in this new small uranium-bearing molecule.

[a] Dr. X. Wang, Prof. Dr. L. Andrews
Department of Chemistry, University of Virginia
P.O. Box 400319, Charlottesville, VA 22904-4319 (USA)
Fax: (+1) 434-924-3710
E-mail: lsa@virginia.edu

[b] Dr. C. J. Marsden
Laboratoire de Chimie et Physique Quantiques, UMR 5626
IRSAMC, Universite Paul Sabatier
118 Route de Narbonne, 31062 Toulouse Cedex 9 (France)

Supporting information for this article is available on the WWW under http://dx.doi.org/10.1002/chem.200800875.

## Experimental and Computational Methods

The application of laser ablation and matrix isolation for infrared spectroscopic identification of new uranium-containing reaction product molecules has been described previously.[16,17,19–21] The Nd:YAG laser fundamental (1064 nm, 10 Hz repetition rate, 10 ns pulse width) was focused on a rotating uranium metal target (Oak Ridge National Laboratory) using 5–20 mJ per pulse. Laser-ablated uranium atoms were co-deposited with $NH_3$ (typically 0.2%, but 0.5 and 0.1% were also employed) in excess argon onto an 8 K CsI window at 2–3 mmol $h^{-1}$. Ammonia (Matheson), $ND_3$ (MSD Isotopes), and $^{15}NH_3$ (Cambridge Isotopic Laboratories) were used in different experiments. Deuterated ammonia was co-deposited directly from the cylinder through a Granville-Phillips leak valve into the argon stream to minimize isotopic exchange with the system (typically, the 830 $cm^{-1}$ $NHD_2$ absorption was 20% of the 760 $cm^{-1}$ $ND_3$ band intensity). The $^{15}NH_3$ sample was exchanged with the sample vacuum system until 80–90% enrichment was achieved. Infrared spectra were recorded at 0.5 $cm^{-1}$ resolution on a Nicolet 550 spectrometer with 0.1 $cm^{-1}$ accuracy by using an HgCdTe detector. Matrix samples were irradiated with a medium-pressure mercury arc lamp (Philips, 175W, globe removed, $\lambda > 220$ nm) using glass filters, and annealed at different temperatures before more spectra were recorded.

As described recently for thorium and ammonia oxidative addition reaction products,[9] density functional theory (DFT) calculations were done for expected uranium and ammonia reaction product molecules by using the Gaussian 03 program system.[22] Standard all-electron triple-zeta basis sets were used for N and H,[23] augmented with polarization functions (d-type exponent 0.75 for N, p-type exponent 0.9 for H), whereas "very small-core" pseudopotentials were adopted for U (60 electrons treated as "core", corresponding to those in atomic orbitals with a principal quantum number of less than 5), together with the associated flexible basis sets.[24] Two different versions of density functional theory were employed: B3LYP[25] and PW91.[26] The "ultrafine" grid was used for all calculations of vibrational frequencies reported here. A few calculations of the coupled-cluster type (CCSD and CCSD(T)) were undertaken,[27] sometimes with geometry optimization, for purposes of comparison. Two g-type functions were added to the uranium basis (exponents 1.5 and 0.5) for these calculations, and excitations out of the 10 lowest-energy occupied orbitals (the corelike 5s, 5p, and 5d on U together with 1s on N) and into their high-energy virtual counterparts were excluded. In these calculations, excitations out of the 10 lowest-energy occupied orbitals and into their virtual counterparts were excluded. Spin contamination was never serious, as the values of S**2 did not exceed the ideal values of 2.0 for a triplet or 6.0 for a quintet by more than 2%.

## Results and Discussion

Laser-ablated U atoms react with $NH_3$ molecules in excess argon to produce two groups of new IR absorptions at 1488.6, 1349.8, and 508.5 $cm^{-1}$ and at 1436.3, 1403.0, 819.9, 495.7, and 459.5 $cm^{-1}$. Figure 1 illustrates the IR spectra. The first group of absorptions (labeled $H_2NUH$) was stronger on sample deposition, and annealing to 20 and 25 K sharpened the absorptions in both groups slightly, but increased markedly a weak new absorption at 1138.2 $cm^{-1}$ (labeled $U{:}NH_3$) and produced a new band at 1102.4 $cm^{-1}$ (labeled $U(NH_3)_2$). Note that sample irradiation with $\lambda > 530$ and $> 470$ nm light from a mercury arc increased the second group (labeled $HNUH_2$) and destroyed the first group and the 1138.2 $cm^{-1}$ feature. Subsequent annealing to 25 K sharpened the second group of absorptions and restored part of the 1138.2 $cm^{-1}$ band. Lower-frequency satellite features increased on annealing at 1429.7, 1417.9, 1390.6, and 1382.0 $cm^{-1}$ and at 1340.8, 1334.4, and 1328.0 $cm^{-1}$.

In the 800 $cm^{-1}$ region, the weak 819.6 $cm^{-1}$ UO absorption[20] contained a distinct 819.9 $cm^{-1}$ shoulder (examined under expanded frequency scale), which was clearly absent with the $^{15}NH_3$ precursor (Figure 2). This 819.9 $cm^{-1}$ shoulder (labeled $HNUH_2$) gave way to an 817.0 $cm^{-1}$ satellite on annealing (labeled $HNUH_2(NH_3)_n$). These two bands were

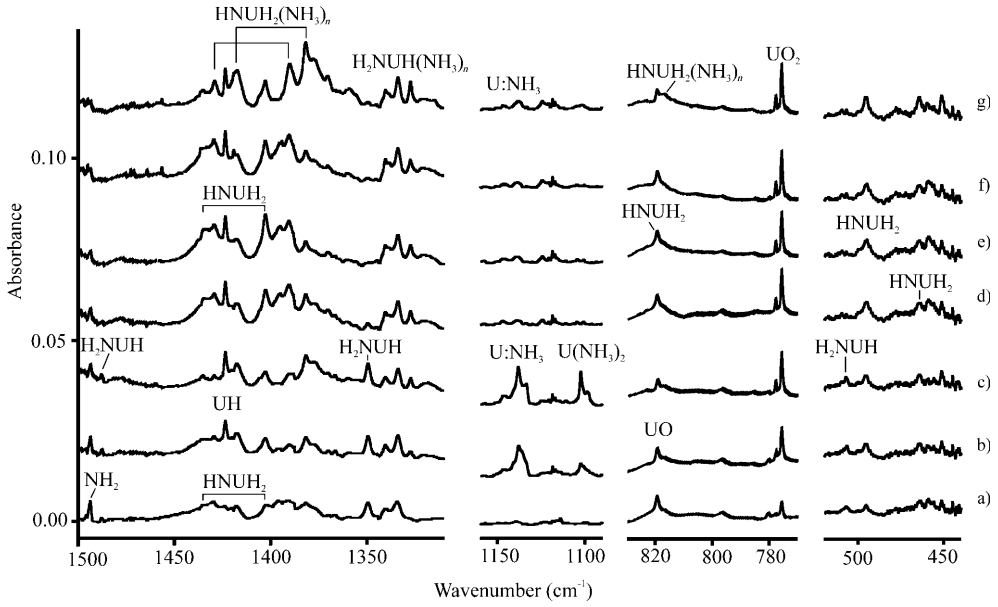


Figure 1. Infrared spectra for uranium and ammonia reaction products in solid argon at 8 K: a) after laser-ablated U atoms were co-deposited with a 0.2% $NH_3$ sample in argon for 60 min, b) after annealing to 20 K, c) after annealing to 25 K, d) after irradiation at $\lambda > 530$ nm for 20 min, e) after irradiation at $\lambda > 470$ nm for 20 min, f) after $\lambda = 240$–380 nm irradiation for 20 min, g) after annealing to 25 K. The band labeled $NH_2$ is common to all ammonia experiments with laser-ablated metal atoms.

  

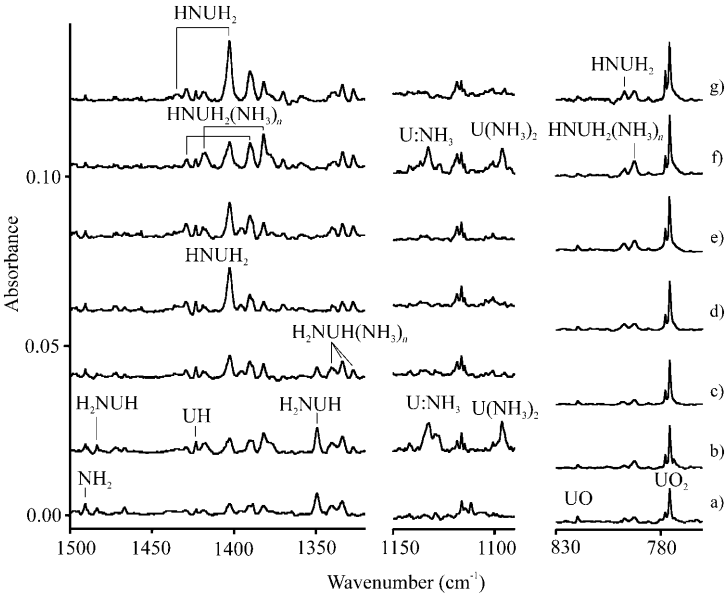


Figure 2. Infrared spectra for uranium and $^{15}NH_3$ reaction products in excess argon at 8 K: a) after laser-ablated U atoms were co-deposited with a 0.5% ammonia sample (>90% nitrogen-15 enrichment), b) after annealing to 20 K, c) after annealing to 25 K, d) after irradiation at $\lambda >$ 530 nm for 20 min, e) after irradiation at $\lambda > 470$ nm for 20 min, f) after $\lambda = 240$–380 nm irradiation for 20 min, g) after annealing to 25 K.

shifted to 797.2 and 792.5 $cm^{-1}$ with the $^{15}NH_3$ precursor. Eight experiments were done with the $^{15}NH_3$ reagent with progressive enrichment exchange with the vacuum system to correlate nitrogen isotopic components of the new product absorptions. In the upper region the only new band to shift (labeled $H_2NUH$) on nitrogen-15 substitution was from 1488.6 to 1483.5 $cm^{-1}$. In the lower region the 508.5 $cm^{-1}$ band gives way on irradiation to absorptions at 495.7 and 459.5 $cm^{-1}$, and annealing increases the 495.7, 465.1, and 451.7 $cm^{-1}$ bands. The spectra in Figure 2 again show the unique chemical behavior of the several product species observed here. The photosensitive $U{:}NH_3$ species is very weak on sample deposition, but it increases on annealing, only to be destroyed on visible irradiation. The first group of bands (labeled $H_2NUH$) gives over to the second group (labeled $HNUH_2$) on visible irradiation, which did not destroy the satellite features (labeled $H_2NUH(NH_3)$). Final annealing restores part of the $U{:}NH_3$ absorption and increases the satellite bands (labeled $HNUH_2(NH_3)_n$).

Spectra from an experiment with lower ammonia concentration (0.1%) and lower laser energy with approximately half of the uranium concentration as used in the Figure 1 experiment are shown in Figure S1 in the Supporting Information. The 1436.3, 1403.0, and 1349.8 $cm^{-1}$ bands are, of course, weaker, and the 1138.2 $cm^{-1}$ band was not detected on sample deposition. In this experiment sequential visible irradiation was employed before annealing, and the 1436.3 and 1403.0 $cm^{-1}$ bands increased at the expense of the 1349.8 $cm^{-1}$ band, but ultraviolet irradiation reversed this change in relative band intensities, and a second $\lambda > 470$ nm irradiation reproduced the original effect. Annealing to 20 K did produce the weak 1138.2 $cm^{-1}$ band, and annealing to 30 K increased the 1103.0 $cm^{-1}$ feature as well as the above-described satellite absorptions for higher complexes, but decreased the initial isolated product absorptions.

The uranium reaction products are weak in these laser-ablation experiments in part because the uranium atom concentration produced by laser ablation is low owing to the refractory nature of uranium metal. Thus, we believe it highly unlikely that two uranium atoms contribute to the major product species. In comparable experiments using Mo, which is easier to ablate than U, the major product species exhibits an Mo–N stretching mode with resolved natural Mo isotopic splittings and confirms the presence of a single Mo atom in this reaction product.[15]

Ammonia is known to diffuse and aggregate readily on annealing matrix samples,[28] and the new satellite features are appropriate for the product coordinated by additional ammonia molecules. A broad band increased on annealing at 1263 $cm^{-1}$, which has been attributed to $(UH)_x$ species in experiments with the $H_2$ reagent.[21] The $NH_2$ radical band at 1495.6 $cm^{-1}$ is common to laser-ablated metal experiments with ammonia.[9,29] Additional weak absorptions were observed at 1423.6 $cm^{-1}$ (UH), and at 819.6 and 775.8 $cm^{-1}$ (UO and $UO_2$ from target surface contamination).[20,21] The very weak $UN_2$ absorption at 1051.1 $cm^{-1}$ ($A = 0.001$) indicates a minimal air leak in our vacuum system as the U and $N_2$ reaction is very favorable.[3] Experiments were done with ammonia concentrations of 0.5, 0.2, and 0.1% in argon, and 0.2% appeared to give the best results though band intensities followed sample concentration as expected. Laser energy was also varied up and down by 50% and the bands within the above absorption groups were tracked together under these changes in reaction conditions. These were among the most difficult experiments to perform under optimum conditions that we have ever done. This is because laser ablation provides heat to the condensing sample and makes it difficult to isolate the rapidly diffusing ammonia precursor molecule. Hence, we found that 12 K was not cold enough and 8 K was required to isolate the simple products of these reactions.

Five new absorptions were observed in four studies with U and $ND_3$, and only one of these, the $ND_2$ radical band at 1107.0 $cm^{-1}$ was observed in similar $ND_3$ experiments with other metals. Group one counterparts appeared at 1104.8 and 964.0 $cm^{-1}$, group two bands were observed at 1024.6 and 1002.5 $cm^{-1}$, and the U ammonia complex band was observed at 883.4 $cm^{-1}$, as shown in Figure 3. Unfortunately, the group two band expected near 790 $cm^{-1}$ was covered by the $(ND_3)_3$ absorption at 792 $cm^{-1}$. As with $NH_3$, the latter complex bands increased on annealing and disappeared on irradiation, which increased group one and particularly group two absorptions.

Following our investigation of Th and $NH_3$ reaction products[9] and that of Zhou et al.[12,13] with Group 4 metal atoms, structure and frequency calculations were performed for $U{:}NH_3$, $H_2N{-}UH$, and $HN{=}UH_2$ at the B3LYP and PW91 levels of theory. Recent work with $CH_3{-}UH$ and $CH_2{=}UH_2$

  

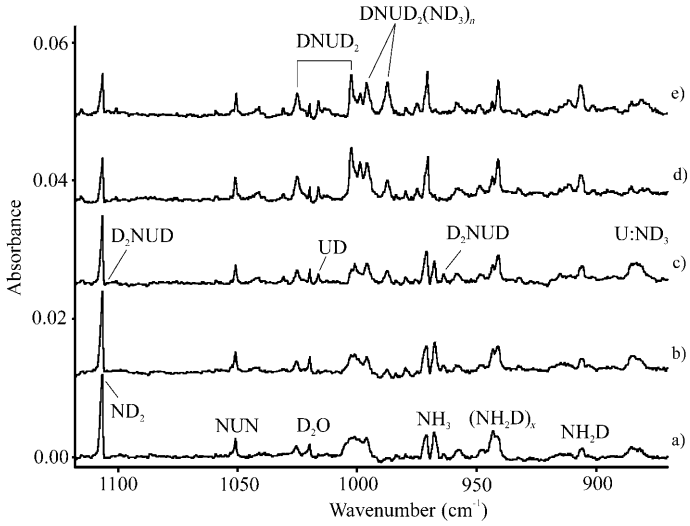


Figure 3. Infrared spectra for uranium and $ND_3$ reaction products in excess argon at 8 K: a) after laser-ablated U atoms were co-deposited with a 0.5% ammonia sample (>90% deuterium enrichment), b) after annealing to 20 K, c) after annealing to 25 K, d) after irradiation at $\lambda >$ 470 nm for 20 min, and e) after annealing to 23 K.

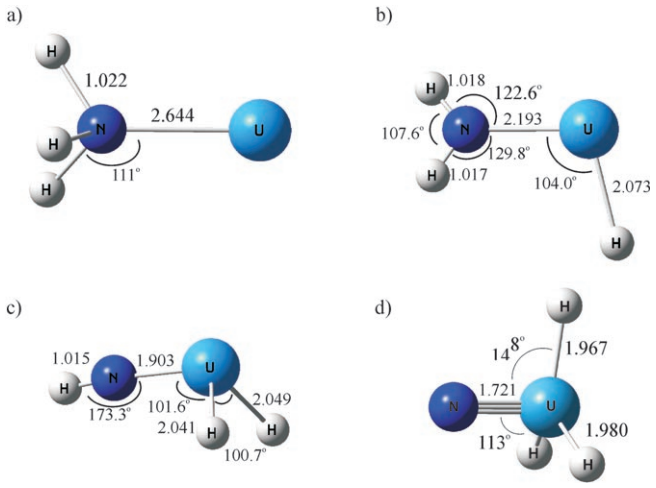


Figure 4. Structures calculated for a) $U{:}NH_3$ ($C_{3v}$), b) $NH_2{-}UH$ ($C_1$), c) $HN{=}UH_2$ ($C_1$), and d) $N{\equiv}UH_3$ ($C_{3v}$) with parameters listed for calculations.

has shown that DFT calculations provide structures comparable to the more rigorous CASPT2 method, even for open-shell species if spin contamination is not serious.[17,18] Computed structures are illustrated in Figure 4. Vibrational frequencies computed for open-shell actinide-containing systems are also generally reliable, in our experience.[4,17] Computed structures and the calculated frequencies are compared in Tables 1 and 2 with observed frequencies that we assign here to the new $H_2N{-}UH$ and $HN{=}UH_2$ molecules in the $^5A$ and $^3A$ ground electronic states, respectively, in $C_1$ symmetry.

**$H_2N{-}UH$**: The strongest absorption by far for the $H_2N{-}UH$ molecule is the U–H stretching mode calculated at 1382.2 (B3LYP) or 1387.8 $cm^{-1}$ (PW91), and the 1349.8 $cm^{-1}$ band with ammonia complex satellites at 1340.8, 1334.4, and 1327.7 $cm^{-1}$ is appropriate for this vibrational fundamental. The calculated frequency is 2.4 (B3LYP) or 2.8% (PW91) high for the isolated molecule, which is the order of agreement expected for DFT calculated harmonic and observed frequencies.[19,30,31] The lack of $^{15}N$ shift and large H/D isotopic frequency ratio (1349.8/964.0 = 1.400) support this assignment. (The satellite absorptions appeared at 1327.5, 1320.7, and 1311.7 $cm^{-1}$ with a different intensity profile in solid krypton, which is appropriate for

Table 1. Comparison of calculated harmonic and observed argon matrix frequencies for the $H_2N{-}UH$ uranium hydride amine.[a]

| $H_2N{-}UH$ | | | $H_2{}^{15}N{-}UH$ | | $D_2N{-}UD$ | | Mode |
|---|---|---|---|---|---|---|---|
| B3LYP | PW91 | observed | B3LYP | observed | B3LYP | observed | description |
| 3557.8 (8) | 3486.1 (7) | –[b] | 3548.0 | – | 2618.6 | – | N–H stretch |
| 3468.2 (16) | 3387.6 (11) | –[b] | 3463.3 | – | 2506.7 | – | a′ N–H stretch |
| 1540.9 (50) | 1484.1 (45) | 1488.6 | 1535.9 | 1483.5 | 1144.5 | 1104.8 | a″ $NH_2$ bend |
| 1382.2 (379) | 1387.8 (320) | 1349.8 | 1382.2 | 1349.8 | 980.1 | 964.0 | a′ U–H stretch |
| 525.9 (97) | 532.9 (75) | – | 511.8 | – | 490.9 | – | a′ N–U stretch |
| 489.4 (124) | 465.7 (108) | 508.5 | 486.3 | 505.4 | 378.4 | – | a″ H-N-U bend |
| 409.5 (29) | 392.9 (30) | – | 407.4 | – | 310.2 | – | a′ $UH_2$ bend |
| 252.0 (45) | 237.2 (34) | – | 251.9 | – | 179.1 | – | a″ $UH_2$ bend |
| 159.2 (21) | 169.1 (15) | – | 159.2 | – | 112.7 | – | a′ $NUH_2$ def[c] |

[a] All calculations used the TZP/SDD basis set, and all frequencies are in $cm^{-1}$. Intensities are in km $mol^{-1}$. The mode description gives the major coordinate, using local symmetry for the $NH_2$ group. [b] Overlapped by precursor band. [c] def = deformation.

Table 2. Comparison of calculated harmonic and observed argon matrix frequencies for the $HN{=}UH_2$ uranimine.[a]

| $HN{=}UH_2$ | | | $H^{15}N{=}UH_2$ | | $DN{=}UD_2$ | | Mode |
|---|---|---|---|---|---|---|---|
| B3LYP | PW91 | observed | B3LYP | observed | B3LYP | observed | description |
| 3558.8 (67) | 3470.4 (47) | –[b] | 3550.1 | – | 2611.9 | – | a′ N–H stretch |
| 1465.2 (358) | 1446.4 (346) | 1436.3 | 1465.1 | 1436.3 | 1041.0 | 1024.6 | a′ $UH_2$ stretch |
| 1420.4 (664) | 1418.8 (540) | 1403.0 | 1420.4 | 1403.0 | 1007.9 | 1002.5 | a″ $UH_2$ stretch |
| 837.9 (276) | 821.0 (240) | 819.9 | 813.7 | 797.2 | 805.6 | –[b] | a′ N=U stretch |
| 520.9(176) | 514.8 (177) | 495.7[c] | 518.1 | 492.9[c] | 397.9 | – | a′ H-N-U bend |
| 483.8 (122) | 486.1 (121) | 459.5 | 481.8 | 456.7 | 368.7 | – | a″ H-N-U bend |
| 471.6 (126) | 473.0 (47) | [465.1][c] | 470.9 | [464.5][c] | 336.0 | – | a′ $UH_2$ bend |
| 316.1(3) | 286.0 (3) | – | 315.6 | – | 228.3 | – | a″ $UH_2$ bend |
| 258.1(178) | 244.6 (150) | – | 257.7 | – | 186.2 | – | a′ $NUH_2$ def[d] |

[a] All calculations used the TZP/SDD basis set, and all frequencies are in $cm^{-1}$. Intensities are in km $mol^{-1}$. The mode description gives the major coordinate, using local symmetry for the $UH_2$ group. [b] Overlapped by precursor band. [c] Contains contribution from product (ammonia complex). The 465.1 and 451.8 $cm^{-1}$ bands are due to this complex. [d] def = deformation.

matrix site splittings.)[9] The weaker 1488.6 $cm^{-1}$ band shows the appropriate $^{15}N$ shift (both B3LYP and PW91 calcd: 5.0 $cm^{-1}$; obsd: 5.1 $cm^{-1}$) and a lower H/D isotopic frequency ratio (1488.6/1104.8 = 1.352) for the $NH_2$ bending mode, which is calculated at 1540.9 (B3LYP, 3.5% high) or 1484.1 $cm^{-1}$ (PW91, 0.3% low). The single photosensitive absorption in the lower region is at 508.5 $cm^{-1}$, and this band shows a 3.1 $cm^{-1}$ $^{15}N$ shift, which characterizes a H-N-U bending mode. Such a mode is calculated at 489.4 (B3LYP) or 465.7 $cm^{-1}$ (PW91), with $^{15}N$ shifts of 3.1 and 3.0 $cm^{-1}$, respectively, and is the strongest band in this region, but it is computed to be only one third of the intensity of the strong U−H stretching mode. Unfortunately the DFT calculations do not perfectly describe the low frequency modes and their mixing for this molecule, and the U−N stretching mode calculated at 525.9 (B3LYP) or 532.9 $cm^{-1}$ (PW91) with a 14.1 (B3LYP) or 14.3 $cm^{-1}$ (PW91) $^{15}N$ shift is not strong enough to be detected here. Finally, the N−H stretching modes are too weak, based on calculated intensity, to be observed in these experiments.

**HN=UH$_2$**: Similarly to $H_2N$−UH, the strongest IR absorptions for the HN=$UH_2$ molecule are the two U−H stretching modes calculated at 1420.4 and 1465.2 (B3LYP) or 1446.4 and 1418.8 $cm^{-1}$ (PW91), which are observed here at 1403.0 and 1436.3 $cm^{-1}$ in solid argon (Table 2). These bands are not displaced with $^{15}N$ but shift to 1024.6 and 1002.5 $cm^{-1}$ on deuteration and show the large H/D isotopic frequency ratios (1.402 and 1.400, respectively) expected for very heavy metal hydride motions ($UH_4$ shows a 1.3987 H/D frequency ratio).[21] The diagnostic absorption for this molecule is the U=N stretching frequency calculated at 837.9 (B3LYP) or 821.0 $cm^{-1}$ (PW91) with a 24.2 (B3LYP) or 23.8 $cm^{-1}$ (PW91) $^{15}N$ shift, and the 819.9 $cm^{-1}$ shoulder (above the 819.6 $cm^{-1}$ UO absorption) with 22.7 $cm^{-1}$ $^{15}N$ shift (Figure 2) confirms this assignment. Lower frequency H-N-U bending modes calculated at 520.9 and 483.8 (B3LYP) or 514.8 and 486.1 $cm^{-1}$ (PW91) are observed at 495.7 and 459.5 $cm^{-1}$, and again, the N−H stretching mode is too weak to be observed in a region filled with precursor absorptions.

The three bond-stretching modes observed here for HN=$UH_2$ are calculated at the B3LYP level to be 2.0, 1.2, and 2.2% higher than the observed argon matrix values, which is very good agreement, slightly better than that found for the analogous thorium imine product.[9] At the PW91 level, the differences are even smaller, at 0.7, 1.1, and 0.1%. The bending region is not predicted quite so well: the differences between B3LYP (PW91) predictions and the observed matrix observations are 5.1, 5.3, and 1.4% (3.9, 5.8, and 1.7%). When the eight observed modes are considered for $H_2N$−UH and HN=$UH_2$ taken together, there is no overall advantage for either of the DFT methods: the average error, taking account of signs, is larger for B3LYP than for PW91 (2.1 compared to 0.8%), but the spread about this mean is smaller for B3LYP (1.7%, compared with 2.4% for PW91). The unsigned average error is almost identical for the two functionals: 3.0% for B3LYP and 2.9% for PW91. These "errors" must be interpreted with care, since they represent the difference between computed harmonic values for the gas phase and observed anharmonic values in argon matrices. Since the differences between these two types of quantities can easily be 1–2%, the real message is that the performance of both functionals is always good, and usually very good, for the prediction of vibrational frequencies. Both functionals give good, if not very good, predictions for the isotopic shifts and there is no systematic preference for one or the other.

The $H_2N$−UH and HN=$UH_2$ molecules are particularly sensitive to formation of complexes with additional ammonia molecules. The U−H stretching modes are most affected, as attested by the several new satellite features that appear below the isolated molecule absorptions assigned above and increase on annealing. This suggests that the point of attachment for the ammonia ligand in this complex is the metal center. One such absorption is observed at 817.0 $cm^{-1}$ below the UO band, and the $^{15}N$ counterpart is at 792.5 $cm^{-1}$ as shown in Figure 2. In the lower frequency region bending modes are observed for the complex at 495.7 (coinciding with absorptions of the isolated molecule), 465.1, and 451.7 $cm^{-1}$. B3LYP calculations located complexes of $NH_3$ with both $H_2N$−UH and HN=$UH_2$, in which the $NH_3$ is indeed bonded to U rather than hydrogen bonded to H(N). The binding in these complexes is calculated to be surprisingly strong, at 65 and 90 kJ $mol^{-1}$, respectively, but the calculated vibrational characteristics do not match those observed: the U−H stretching modes are predicted to decrease substantially, by 50–125 $cm^{-1}$, while gaining intensity.

**U:NH$_3$**: The U:$NH_3$ complex is characterized by a single absorption at 1138.2 $cm^{-1}$, and its 5.9 $cm^{-1}$ isotopic $^{15}NH_3$ shift to 1132.3 $cm^{-1}$ and large deuterium shift to 883.4 $cm^{-1}$ with H/D ratio of 1.288. These shifts may be compared to those observed for the $NH_3$ monomer itself in solid argon ($^{15}N$ shift of 4.2 $cm^{-1}$ and H/D ratio 1.282).[28] Our calculations for U:$NH_3$ predict one very strong absorption at 1175 (B3LYP) or 1129 $cm^{-1}$ (PW91) corresponding to the very strong ammonia umbrella bending mode, which is calculated at 1000 (B3LYP) or 989 $cm^{-1}$ (PW91) for ammonia itself. The calculated wavenumbers are 2.7 (B3LYP) or 1.5% (PW91) too high for ammonia itself and 3.2% high (B3LYP) or 0.8% low (PW91) for the U:$NH_3$ complex and the predicted $^{15}N$ shifts of 6.5 (B3LYP) or 6.6 $cm^{-1}$ (PW91) are slightly higher than our observed value. The increase in $^{15}N$ shift in U:$NH_3$ over $NH_3$ itself (0.52% of the vibrational wavenumber, compared to 0.43%) is due to increased N motion in this mode between the three H atoms and the U center. The 1138.2 $cm^{-1}$ absorption for the U:$NH_3$ complex may be compared to the 1149.0 $cm^{-1}$ measurement for Th:$NH_3$, the 1158.8 $cm^{-1}$ frequency for Hf:$NH_3$, and the 1188.0 $cm^{-1}$ value for W:$NH_3$.[9,13,15]

The U$(NH_3)_2$ complex absorption at 1102.4 $cm^{-1}$ shifts to 1096.5 $cm^{-1}$ with $^{15}N$, but the D counterpart was masked. Higher $NH_3$ complexes such as U$(NH_3)_2$ and U$(NH_3)_3$ were

  

studied at the B3LYP level of theory. The binding energy for the dimer compared with the monomer is surprisingly high, at 74 kJ mol$^{-1}$, whereas the trimer is bound by 41 kJ mol$^{-1}$ compared with the dimer. The dimer is predicted to be essentially linear at U, but the intense umbrella mode is only 11 cm$^{-1}$ lower than that for the monomer, an appreciably smaller shift than that observed (36 cm$^{-1}$). We also studied species containing an $NH_3$ group linked to the $NH_3$ in U:$NH_3$ by a hydrogen bond, rather than two $NH_3$ groups both linked to U. A true minimum was found ($C_1$ symmetry), bound by 39 kJ mol$^{-1}$ (with respect to U:$NH_3$+$NH_3$) at the B3LYP level. However, the IR spectra predicted for this species (intense "umbrella" modes 82 cm$^{-1}$ higher and 67 cm$^{-1}$ lower than those for U:$NH_3$) do not match that observed and the exact nature of the observed higher complex species remains unclear.

**N≡UH$_3$**: The N≡$UH_3$ molecule is an isomer of $H_2N$–UH and HN=$UH_2$ and is especially interesting due to its formal triple bond, but there is no experimental evidence for its formation in our experiments. Its spectroscopic detection would be straightforward, since it has a characteristic strong N≡U stretching motion in the region near 1050 cm$^{-1}$ that is not obscured by other products or initial reagents. We note that uranium compounds in the +6 oxidation state are not stable unless very electronegative ligands are present. For example, the decomposition of $UH_6$ to $UH_4$+$H_2$ is calculated to be exothermic by 239 kJ mol$^{-1}$[32] and $UH_6$ is not observed in reactions of atomic U with dihydrogen[21a] in circumstances similar to those in which $WH_6$ is readily formed.[33,34] In addition, the HC≡$UH_3$ molecule is high energy, but the HC≡$UF_3$ molecule is stable and observable.[17,35]

The triple-bond length in N≡$UH_3$ is calculated to be 1.721 Å, precisely that predicted from triple-bond radii.[36] Thus, the instability of the N≡$UH_3$ molecule arises from the lack of electronegative elements to stabilize the VI state, and the weakness of the U–H bonds relative to N–H bonds. Consistent with this conclusion, N≡$UF_3$ has recently been prepared in reactions between laser-ablated uranium atoms and $NF_3$,[7] in which the combination of very strong U–F bonds and weak N–F bonds makes the triple-bonded species much more energetically favorable. The bonding in these compounds is discussed in the section below.

It is interesting to note here that the reaction of Mo and W atoms with ammonia recently investigated in this laboratory passes through the HN=$MH_2$ intermediate directly to the lower-energy N≡$MH_3$ molecules. In this case the Mo–H and W–H bonds are relatively stronger than the U–H bond, and the final terminal nitride product is produced with Mo and W.[15]

**Analysis of the bonding**: We now turn to an analysis of the bonding in these new compounds containing U–N bonds. The data in Tables 3 and 4 support several pertinent geometrical and thermochemical comparisons. For convenience and consistency, all the data in Table 4 were obtained at the B3LYP level of theory, using basis sets equivalent to those described here for U, N, and H, even though results for several of those compounds have already appeared in the literature.[16–19,35] We shall also comment on the natural bond orbital (NBO) analysis[37] of these compounds and analyze several individual MOs of the analogous Th and U compounds (HN=$ThH_2$ and HN=$UH_2$). We are particularly interested in discovering whether the formal An–N and An=N bonds (An = Th, U) are shorter and stronger than might be expected, based on the properties of related compounds. We also wish to quantify the possible differences in properties of the analogous Th–N/U–N and Th=N/U=N bond pairs.

Table 3. Electronic binding energies (BE in kJ mol$^{-1}$) relative to U+$NH_3$[a] and U–N bond lengths ($r$(U–N) in Å) obtained with four different theoretical methods.

| Compound | | B3LYP | PW91 | CCSD | CCSD(T)[b] |
|---|---|---|---|---|---|
| U:$NH_3$ | BE | 52.4 | 82.6 | 31.3 | 40.2 |
| | $r$(U–N) | 2.644 | 2.554 | 2.605 | – |
| $H_2N$–UH | BE | 193.7 | 217.6 | 165.5 | 166.1 |
| | $r$(U–N) | 2.193 | 2.166 | 2.187 | – |
| HN=$UH_2$ | BE | 178.0 | 226.2 | 165.4 | 185.3 |
| | $r$(U–N) | 1.903 | 1.898 | 1.891 | – |
| N≡$UH_3$ | BE | 26.5 | 131.7 | 29.2 | 75.3 |
| | $r$(U–N) | 1.721 | 1.741 | 1.706 | – |

[a] Positive values indicate compounds more stable than U+$NH_3$. [b] CCSD(T) results at optimized CCSD geometries.

Table 4. Structural and thermochemical data.[a]

| Compound | Bond length [Å] | Bond energy [kJ mol$^{-1}$] |
|---|---|---|
| $NH_2$–UH | 2.193 | 380 |
| NH=$UH_2$ | 1.903 | 524 |
| N≡$UH_3$ | 1.721 | 437 |
| N≡UH | 1.760 | 554 |
| $CH_3$–UH | 2.395 | 237 |
| $CH_2$=$UH_2$ | 2.053 | 379 |
| CH≡$UH_3$ | 1.899 | 324 |
| CH≡UH | 1.915 | 501 |
| $NH_2$–ThH | 2.176 | 446 |
| NH=$ThH_2$ | 1.951 | 620 |
| N≡ThH | 1.820 | 628 |
| $CH_3$–ThH | 2.400 | 292 |
| $CH_2$=$ThH_2$ | 2.117 | 470 |
| CH≡ThH | 1.978 | 564 |
| $NH_2$–WH | 1.974 | 329 |
| NH=$WH_2$ | 1.737 | 516 |
| N≡$WH_3$ | 1.660 | 644 |
| N≡WH | 1.660 | 600 |
| $CH_3$–WH | 2.062 | 181 |
| $CH_2$=$WH_2$ | 1.878 | 459 |
| CH≡$WH_3$ | 1.739 | 648 |
| CH≡WH | 1.747 | 592 |
| $NH_2$–HfH | 1.998 | 449 |
| NH=$HfH_2$ | 1.813 | 582 |
| N≡HfH | 1.738 | 511 |
| $CH_3$–HfH | 2.161 | 298 |
| $CH_2$=$HfH_2$ | 1.959 | 455 |
| CH≡HfH | 1.861 | 503 |

[a] B3LYP geometries, bond dissociation energies [kJ mol$^{-1}$] from energies of fragments (see text).

  

The data in Table 3 enable us to compare the thermodynamic stabilities of the four isomeric species $H_3N{:}U$, $H_2N{-}UH$, $HN{=}UH_2$, and $N{\equiv}UH_3$, in which uranium is in the oxidation states 0, +2, +4, and +6, respectively (but we note that spin-orbit effects have been neglected here and their influence on relative energies may not be negligible). The stabilities of $H_2N{-}UH$ and $HN{=}UH_2$ are similar: depending on the theoretical method chosen, the imine is either slightly lower (CCSD(T) and PW91) or slightly higher (B3LYP) in energy than the amine, with the CCSD method finding them almost degenerate. The triple-bonded molecule $N{\equiv}UH_3$ is substantially higher in energy than $H_2N{-}UH$ or $HN{=}UH_2$, but its stability relative to the $NH_3$ adduct varies appreciably according to the theoretical method used. The CCSD(T) binding energies should be the most reliable of those reported in Table 3. Since the values of the CCSD T1 diagnostic for $HN{=}UH_2$ and $H_2N{-}UH$ are not excessively high, at 0.033 and 0.027, respectively, single-reference methods such as CCSD(T) should be appropriate. We observe that the PW91 functional leads to stronger binding than the other methods, as is often observed for GGA functionals in actinide chemistry.[38] For $H_3N{:}U$, $H_2N{-}UH$, and $HN{=}UH_2$, the B3LYP binding energies are fairly close to those obtained at the CCSD(T) level.

Even though bond dissociation energies (BDE) are surely of greater fundamental significance than bond lengths, we discuss the latter before the former, since evidence is emerging that spin-orbit effects on ground-state geometries are weak, even for open-shell systems,[39] and the good performance of DFT methods for geometry prediction is well established.[40] The most striking aspect of the geometry of $HN{=}UH_2$ concerns the length of the U=N bond (see Figure 4), which is 0.145 Å shorter than the U−H bonds in the same compound, and no less than 0.290 Å shorter than the single U−N bond in $H_2N{-}UH$. We consider first these bond lengths "from first principles", neglecting for the moment the experimental results available for the imido species.[1]

Using the concept of covalent radii, an extrapolation from the C=N and N−H distances in $HN{=}CH_2$ (1.266 and 1.024 Å, respectively, at the B3LYP level) suggests that the U=N bond in $HN{=}UH_2$ is as much as 0.31 Å shorter "than expected": this value is obtained by adding the difference between C=N and N−H to that between the U=N and N−H distances, noting that the two differences have opposite signs. If the relative electronegativities of U, C, and N are taken into account, the "expected" length of the U=N bond is reduced, but only by 0.09 Å. More realistic bond-length comparisons are provided by $HN{=}WH_2$, in which the W=N bond is only 0.03 Å shorter than the W−H bonds, or $CH_2{=}UH_2$, in which the U=C bond is 0.02 Å longer than the U−H bonds. These considerations confirm that the U=N bond in $HN{=}UH_2$ is indeed strikingly short.

However, it is clear that N−M and N=M bonds are likely to be substantially shorter and stronger than their C−M and C=M counterparts, if M is a metal with empty orbitals that can accept donation of electron density from formal lone pairs on N. We now use the structural data in Table 4 to quantify this effect for metals from the third row of the transition series, the examples that provide the best model for the actinide compounds under discussion here. We find that N−Hf and N−W bonds are 0.13–0.14 Å shorter than their C−Hf or C−W counterparts, whereas the analogous shortenings for N−Th and N−U are substantially greater, at 0.20 or 0.22 Å. The data in Table 4 therefore show that the formal single U−N bond in $H_2N{-}UH$ is indeed shorter than might reasonably be expected, by 0.07–0.08 Å. But when we compare the C=Hf/N=Hf and C=W/N=W bond pairs with their actinide analogues, we find that the decrease in length between C=Th and N=Th of 0.166 Å (or between C=U and N=U, 0.150 Å) is scarcely larger than that between C=Hf and N=Hf (0.133 Å) or that between C=W and N=W (0.141 Å). Similarly, the triple bonds between N and Th or U show essentially the same contraction compared to triple bonds between C and Th or U as do the analogous pairs with Hf and W. In other words, the formally single N−An, formally double N=An, and formally triple N≡An bonds are all shorter than might be expected, but by essentially the same amount: the N=U and N≡U bonds in $HN{=}UH_2$ or in $N{\equiv}UH_3$ are of course shorter than U−N in $H_2N{-}UH$, but by amounts that are consistent with the computational data available for related compounds.

We now compare the system studied here with the imido species of the type $U(NR)_2I_2(THF)_2$, which have been synthesized and characterized by Boncella and co-workers.[1] The U=N bond lengths in these compounds of around 1.85 Å found by X-ray diffraction and by B3LYP computations are substantially shorter than the value of 1.903 Å calculated here for $HN{=}UH_2$. However, the oxidation state of uranium in the imido species is +6, whereas in $HN{=}UH_2$ it is +4. To compare systems that are more similar, we have undertaken B3LYP calculations on $U(NH)_2^{2+}$, $U(NH)_2^{+}$, $U(NH)_2$, $U(NH)_3$, and $U(NH)_2F_2$. The optimized U−N distances are 1.761, 1.853, 1.949, 1.928, and 1.868 Å, respectively. These results show that the lengths of formally double U=N bonds are *very* sensitive to the environment and oxidation state of uranium, even more so than for the analogous U−O bonds in the uranyl ion and its reduced derivatives.[4] Detailed comparison of $HN{=}UH_2$ with $U(NR)_2I_2(THF)_2$ is therefore not straightforward.

There is some evidence in Table 4 to suggest that the N−An multiple bonds are particularly strong. It is well known that the bonds formed by atoms of a given group weaken, in general, on descending the periodic table, since compact orbitals overlap more effectively than diffuse ones. Since the actinide atoms are larger than those in the third row of the transition series with the same number of valence electrons, we might expect C−Hf bonds to be stronger than C−Th, C−W to be stronger than C−U, N=Hf to be stronger than N=Th, and so forth. If the N=An bonds in $NH{=}ThH_2$ and $NH{=}UH_2$ are anomalously strong, then the difference between the BDE for N=Th and N=Hf will be less negative (or more positive) than that between C=Th and C=Hf. That is exactly what we find for all four multiple bonds involving N: for the

  

comparisons of N=Th, N≡Th, N=U, and N≡U with their C counterparts, the differences in favor of the N-bonded species are 23, 56, 88, and 45 kJ mol$^{-1}$, respectively.

Do the bond dissociation energies in Table 4 imply that the N−Th and N−U bonds are anomalously strong? The analysis is complicated by the agostic interactions that are present in some of the compounds, the influence of which will contaminate the bond dissociation energies evaluated here (note that agostic interactions have little effect on C=M distances[41]). The N−Hf and N−W bonds are stronger than their C−Hf and C−W counterparts by 151 or 148 kJ mol$^{-1}$, respectively. Very similar increases in bond energies are found for the actinide systems: N−Th (N−U) is stronger than C−Th (C−U) by 154 kJ mol$^{-1}$ (143 kJ mol$^{-1}$). The N=Hf and N=W bonds are stronger than their C=Hf and C=W counterparts by 148 or 57 kJ mol$^{-1}$, respectively, whereas N=Th (N=U) is stronger than C=Th (C=U) by 150 kJ mol$^{-1}$ (145 kJ mol$^{-1}$). Finally, both the N≡Hf and N≡W bonds are stronger than their C≡Hf and C≡W counterparts by 8 kJ mol$^{-1}$, whereas N≡Th (N≡U) is stronger than C≡Th (C≡U) by 64 kJ mol$^{-1}$ (53 kJ mol$^{-1}$). To avoid difficulties associated with changes in oxidation state, we have compared triple bonds to W and U in systems in which these atoms are in the oxidation state +4, like Hf and Th. Note that the dissociation energies of the C≡U and N≡U bonds in CH≡$UH_3$ and N≡$UH_3$ are smaller than those of their counterparts in the $U^{IV}$ compounds by substantial margins (117 kJ mol$^{-1}$ for CH≡$UH_3$ and 177 kJ mol$^{-1}$ for N≡$UH_3$), reflecting the instability of $U^{IV}$ when attached to ligands that are not very electronegative.

At first sight, these bond dissociation energies therefore provide little evidence for anomalously strong bonds between N and either Th or U. But another type of comparison provides more insight. It is well known that the bonds formed by atoms of a given family group weaken, in general, on descending the periodic table, since compact orbitals overlap more effectively than diffuse ones. Since the actinide atoms are larger than those in the third row of the transition series with the same number of valence electrons, we might expect C−Hf bonds to be stronger than C−Th, C−W to be stronger than C−U, N=Hf to be stronger than N=Th, and so forth. If the N=An bonds in NH=$ThH_2$ and NH=$UH_2$ really are anomalously strong, then the difference between the dissociation energies for N=Th and N=Hf will be less negative (or more positive) than that between C=Th and C=Hf. That is exactly what we find for all four multiple bonds involving N: for the comparisons of N=Th, N≡Th, N=U, and N≡U with their C counterparts, the differences in favor of the N-bonded species are 23, 56, 88, and 45 kJ mol$^{-1}$, respectively. For the two single bonds involving N, these comparisons are inconclusive, since the change in bond energy between N−Tm (Tm = Hf, W) and N−An is almost the same as that between C−Tm and C−An.

The angular properties of HN=$UH_2$ are striking: the U-N-H group is almost linear (bond angle 172°), whereas the W-N-H angle in HN=$WH_2$ is 151°. The latter is planar, like $CH_2$=NH, whereas the H-N-U group in HN=$UH_2$ almost bisects the $UH_2$ group. There are therefore essentially two equivalent π-type orbitals on NH that can interact with empty orbitals on U, as shown by Hay in his analysis of imido complexes of U in the +6 oxidation state.[42]

We now compare the N−U and N=U bonds described here with their N−Th and N=Th analogues in $H_2$N−ThH and HN=$ThH_2$. Since the thermodynamic stabilities of $H_2$N−UH and HN=$UH_2$ are similar, whereas HN=$ThH_2$ is about 50 kJ mol$^{-1}$ more stable than $H_2$N−ThH,[9] it might appear that the formal double bond in HN=$UH_2$ is weaker than that in HN=$ThH_2$. However, a more careful energetic analysis leads to a different conclusion: the N=U bond is in fact stronger than might have been expected. Several comparisons show that $U^{IV}$ is generally less stable relative to $U^{II}$ than is $Th^{IV}$ compared to $Th^{II}$. For example, the formation of $ThH_4$ from $ThH_2+H_2$ is exothermic by 186 kJ mol$^{-1}$ (B3LYP), whereas the analogous formation of $UH_4$ is exothermic by only 44 kJ mol$^{-1}$. The $U^{II}$ compound $CH_3$−UH is 97 kJ mol$^{-1}$ more stable than $CH_2$=$UH_2$ (B3LYP), but the $Th^{II}$ compound $CH_3$−ThH is only 9 kJ mol$^{-1}$ more stable than its $Th^{IV}$ isomer. In the light of these data, the $U^{IV}$ imine HN=$UH_2$ could be expected to be about 90 kJ mol$^{-1}$ less stable relative to $H_2$N−UH than HN=$ThH_2$ is compared to $H_2$N−ThH. In fact, the thermodynamic stabilities of $H_2$N−UH and HN=$UH_2$ are similar (within the margin of uncertainty of B3LYP calculations), which implies that HN=$UH_2$ is 30–50 kJ mol$^{-1}$ *more* stable than anticipated.

NBO analysis suggests that the "U=N" bond in HN=$UH_2$ is in fact a triple bond, immediately accounting for the remarkably short U=N distance already noted. But this does not explain the substantial difference between the N=U and N≡U bond lengths of 0.14 Å (see Table 4). The "triple" bond found in the NBO analysis of HN=$UH_2$ is very heavily polarized towards the N atom, with orbitals on U contributing only 15%: in other words, there is extensive lone-pair donation from N to U and the triple-bond description is misleading. In species with a formal triple bond, such as N≡$UH_3$, the bonding is more covalent, with orbitals on U contributing 35%: the resulting interaction leads to a far shorter and stiffer bond. The notion of lone-pair donation helps us to understand why the bond shortening found for An−N compared to An−C is maintained but not increased for An=N compared with An=C, as noted above: a single extra bonding interaction is present in both cases for the species involving N.

Although the NBO analyses of HN=$UH_2$ and HN=$ThH_2$ suggest that the multiple bonding in the two species is similar, there are some small differences. The bonding is a little more covalent for U than for Th, with actinide contributions of 15 and 11%, respectively. As might be expected from the differences in ground-state electronic configurations, the f-type orbitals play a more important role for U than for Th. In HN=$UH_2$, f-type and d-type orbitals on U contribute almost equally, with 49 and 46% of the bonding character, respectively, whereas in HN=$ThH_2$ the corresponding contributions are 31 and 62%. However, we suggest that these figures be interpreted with caution, since they depend appreci-

  

ably on the functional used: with PW91, the f-type character in $HN{=}UH_2$ increases to 59 instead of 49% with B3LYP.

Several molecular orbitals for $HN{=}UH_2$ and $HN{=}ThH_2$ are shown in Figure 5. We present the HOMO−4, HOMO−3, and HOMO−2 for $HN{=}ThH_2$ and the analogous orbitals for $HN{=}UH_2$, which contains two unpaired electrons in essentially f-type orbitals. These are the orbitals that correspond most closely to the σ and two π bonds found by the NBO analyses. The nature of the orbitals is more easily grasped for $HN{=}ThH_2$ than for $HN{=}UH_2$, since there is a plane of symmetry in the former that bisects the $ThH_2$ group. The MOs 16 and 17 have a′ symmetry for $HN{=}ThH_2$, whereas MO 18 is antisymmetric. Although the appearance of the MO for $HN{=}UH_2$ is complicated by the lack of symmetry, the plots do show a little more π-type overlap for the uranium compound, consistent with the slightly greater covalent character revealed by the NBO analysis. It is clear that the Lewis representation $HN{=}AnH_2$ is not really appropriate, since there are two MOs that are almost degenerate, a consequence of the near-linearity of the An-N-H subunit, as noted above.

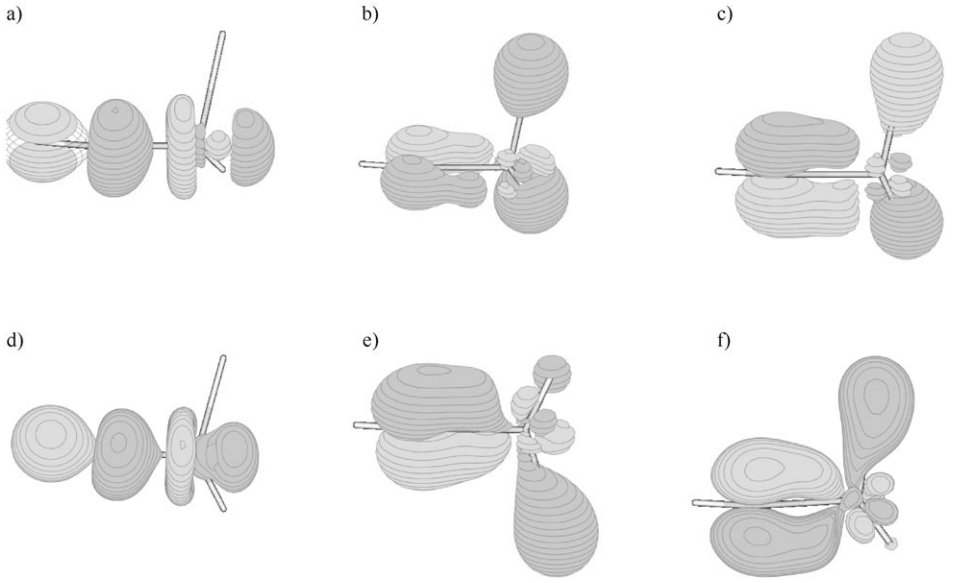


Figure 5. Contour plots comparing the bonding σ and π molecular orbitals in $HN{=}ThH_2$ and $HN{=}UH_2$: a)–c) MO 16–18 of $HN{=}ThH_2$, respectively; d)–f) MO 16–18 of $HN{=}UH_2$, respectively.

## Conclusion

The proposed reaction mechanism is summarized below in Equation (1):

$$U + NH_3 \rightarrow U:NH_3 \rightarrow H_2N{-}UH \rightarrow HN{=}UH_2 \not\rightarrow N{\equiv}UH_3 \quad (1)$$

All of the product absorptions were weak on sample deposition with laser-ablated uranium atoms and ammonia in excess argon. In addition, the $U{:}NH_3$ complex was formed spontaneously on annealing to 20 and 25 K, as found for the thorium, Group 4, and Group 6 metal complexes,[9,12,13,15] and the $H_2N{-}UH$ complex increased 10–20% whereas the $HU{=}UH_2$ complex was unchanged. In contrast, the analogous thorium complexes $H_2N{-}ThH$ and $HN{=}ThH_2$ increased substantially on this annealing process. However, the photochemistry is parallel: the imine species for both actinide metals increased at the expense of the initial metal–ammonia complex and the first group of product absorptions. In addition all of these reaction products form additional complexes with one or more ammonia molecules on annealing of the matrix sample.

There are noteworthy differences between the early actinide metals thorium and uranium, which we have reacted with numerous small molecules.[3,4,8,19–21,43,44] First, thorium is more reactive than uranium in bond activation. This is demonstrated in the $CH_4$ and $CH_3X$ systems[16,17,19,45,46] and is shown again by reactions with ammonia. The spontaneous reaction of Th and $NH_3$ proceeds through the $ThNH_3$ and $H_2N{-}ThH$ intermediates, which are also observed, to the lowest energy final product $HN{=}ThH_2$. The reaction steps are sufficiently exothermic to overcome any energy barriers to the final thorimine product.[9] In contrast, the stable intermediate $U{:}NH_3$ is formed first and photochemically rearranges through $H_2N{-}UH$ to the $HN{=}UH_2$ product. The latter have comparable energies (B3LYP without spin-orbit effects), but visible light irradiation decreases $H_2N{-}UH$ and increases $HN{=}UH_2$, which is a reversible process, and it further shows that this photochemical activation surpasses any barriers to their formation. The low yield of the $U{:}NH_3$ complex on sample deposition is most likely due to photochemical rearrangement by the laser-ablation plume, as found for the analogous Th and Group 4 species.[9,12,13] Since annealing is conducted in the dark, photosensitive species have a high probability of survival.

The structures and energetics of these compounds have been extensively analyzed. Detailed comparisons are presented of the An−N and An=N bonds with analogous bonds to carbon and nitrogen in other systems containing both actinides and third-row transition metals. The An−N and An=N bonds described here are remarkably short, and are substantially stronger than their An−C and An=C counterparts. The 5f and 6d orbitals play a vital role for enhancement of the π bonding in both the amine and imine complexes for

  

both actinide metals. NBO analyses imply that the contributions of the 5f and 6d orbitals are comparable for U, whereas 6d is about twice as important as 5f for Th.

## Acknowledgement

We gratefully acknowledge financial support for this research from the National Science Foundation (U.S.).

[1] a) T. W. Hayton, J. M. Boncella, B. L. Scott, P. D. Palmer, E. R. Batista, P. J. Hay, *Science* **2005**, *310*, 1941; b) T. W. Hayton, J. M. Boncella, B. L. Scott, P. D. Palmer, E. R. Batista, P. J. Hay, *J. Am. Chem. Soc.* **2006**, *128*, 10549.
[2] D. W. Green, G. T. Reedy, *J. Chem. Phys.* **1976**, *65*, 2921.
[3] R. D. Hunt, J. T. Yustein, L. Andrews, *J. Chem. Phys.* **1993**, *98*, 6070.
[4] a) M. F. Zhou, L. Andrews, N. Ismail, C. Marsden, *J. Phys. Chem. A* **2000**, *104*, 5495; b) L. Gagliardi, G. La Manna, B. O. Roos, *Faraday Discuss.* **2003**, *124*, 63.
[5] L. Gagliardi, P. Pyykkö, *Angew. Chem.* **2004**, *116*, 1599; *Angew. Chem. Int. Ed.* **2004**, *43*, 1573.
[6] W. J. Evans, S. A. Kozimor, J. W. Ziller, *Science* **2005**, *309*, 1835.
[7] U + $NF_3$: L. Andrews, X. Wang, R. Lindh, B. O. Roos, C. J. Marsden, *Angew. Chem.* **2008**, *120*, 5446; *Angew. Chem. Int. Ed.* **2008**, *47*, 5366.
[8] C. Burns, *Science* **2005**, *309*, 1823.
[9] Th + $NH_3$: X. Wang, L. Andrews, C. Marsden, *Chem. Eur. J.* **2007**, *13*, 5601.
[10] R. Pearson, F. Lovas, *J. Chem. Phys.* **1977**, *66*, 4149.
[11] O. De Oliveira, J. M. L. Martin, I. K. C. Silwel, J. F. Liebman, *J. Comput. Chem.* **2001**, *22*, 1297.
[12] M. Chen, H. Lu, J. Dong, L. Miao, M. Zhou, *J. Phys. Chem. A* **2002**, *106*, 11456.
[13] M. Zhou, M. Chen, L. Zhang, H. Lu, *J. Phys. Chem. A* **2002**, *106*, 9017.
[14] K. J. De Almeida, A. Cesar, *Organometallics* **2006**, *25*, 3407.
[15] (Cr, Mo, or W) + $NH_3$: X. Wang, L. Andrews, *Organometallics* **2008**, *27* in press.
[16] Th + $CH_4$: L. Andrews, H.-G. Cho, *J. Phys. Chem. A* **2005**, *109*, 6796.
[17] U + $CH_4$: J. T. Lyon, L. Andrews, P.-Å. Malmqvist, B. O. Roos, T. Yang, B. E. Bursten, *Inorg. Chem.* **2007**, *46*, 4917.
[18] M + $CH_4$: B. O. Roos, R. Lindh, H.-G. Cho, L. Andrews, *J. Phys. Chem. A* **2007**, *111*, 6420.
[19] Review article: L. Andrews, H.-G. Cho, *Organometallics* **2006**, *25*, 4040.
[20] U + $O_2$: R. D. Hunt, L. Andrews, *J. Chem. Phys.* **1993**, *98*, 3690.
[21] a) U + $H_2$: P. F. Souter, G. P. Kushto, L. Andrews, M. Neurock, *J. Am. Chem. Soc.* **1997**, *119*, 1682; b) see also: L. Andrews, *Chem. Soc. Rev.* **2004**, *33*, 123.
[22] Gaussian 03, Revision B.04, M. J. Frisch, G. W. Trucks, H. B. Schlegel, G. E. Scuseria, M. A. Robb, J. R. Cheeseman, J. A. Montgomery, Jr., T. Vreven, K. N. Kudin, J. C. Burant, J. M. Millam, S. S. Iyengar, J. Tomasi, V. Barone, B. Mennucci, M. Cossi, G. Scalmani, N. Rega, G. A. Petersson, H. Nakatsuji, M. Hada, M. Ehara, K. Toyota, R. Fukuda, J. Hasegawa, M. Ishida, T. Nakajima, Y. Honda, O. Kitao, H. Nakai, M. Klene, X. Li, J. E. Knox, H. P. Hratchian, J. B. Cross, V. Bakken, C. Adamo, J. Jaramillo, R. Gomperts, R. E. Stratmann, O. Yazyev, A. J. Austin, R. Cammi, C. Pomelli, J. W. Ochterski, P. Y. Ayala, K. Morokuma, G. A. Voth, P. Salvador, J. J. Dannenberg, V. G. Zakrzewski, S. Dapprich, A. D. Daniels, M. C. Strain, O. Farkas, D. K. Malick, A. D. Rabuck, K. Raghavachari, J. B. Foresman, J. V. Ortiz, Q. Cui, A. G. Baboul, S. Clifford, J. Cioslowski, B. B. Stefanov, G. Liu, A. Liashenko, P. Piskorz, I. Komaromi, R. L. Martin, D. J. Fox, T. Keith, M. A. Al-Laham, C. Y. Peng, A. Nanayakkara, M. Challacombe, P. M. W. Gill, B. Johnson, W. Chen, M. W. Wong, C. Gonzalez, J. A. Pople, Gaussian, Inc., Wallingford CT, **2004**, and references therein.
[23] T. H. Dunning, *J. Chem. Phys.* **1971**, *55*, 716.
[24] W. Küchle, M. Dolg, H. Stoll, H. Preuss, *J. Chem. Phys.* **1994**, *100*, 7535.
[25] a) C. Lee, E. Yang, R. G. Parr, *Phys. Rev. B* **1988**, *37*, 785; b) A. D. Becke, *J. Chem. Phys.* **1993**, *98*, 5648.
[26] J. P. Perdew, J. A. Chevary, S. H. Vosko, K. A. Jackson, M. R. Pederson, D. J. Singh, C. Fiolhais, *Phys. Rev. B* **1992**, *46*, 6671.
[27] G. D. Purvis, R. J. Bartlett, *J. Chem. Phys.* **1982**, *76*, 1910.
[28] S. Suzer, L. Andrews, *J. Chem. Phys.* **1987**, *87*, 5131.
[29] D. E. Milligan, M. Jacox, *J. Chem. Phys.* **1965**, *43*, 4487.
[30] A. P. Scott, L. Radom, *J. Phys. Chem.* **1996**, *100*, 16502.
[31] M. P. Andersson, P. L. Uvdal, *J. Phys. Chem. A* **2005**, *109*, 3937.
[32] M. Straka, M. Patzschke, P. Pyykkö, *Theo. Chem. Acta* **2003**, *109*, 332.
[33] $WH_6$: X. Wang, L. Andrews, *J. Am. Chem. Soc.* **2002**, *124*, 5636.
[34] $WH_6$: X. Wang, L. Andrews, *J. Phys. Chem. A* **2002**, *106*, 6720.
[35] U + $CHF_3$: J. T. Lyon, H.-S. Hu, L. Andrews, J. Li, *Proc. Natl. Acad. Sci. USA* **2007**, *104*, 18919.
[36] Triple-bond covalent radii: P. Pyykkö, S. Riedel, M. Patzschke, *Chem. Eur. J.* **2005**, *11*, 3511.
[37] A. E. Reed, L. A. Curtiss, F. Weinhold, *Chem. Rev.* **1988**, *88*, 899.
[38] a) E. R. Batista, R. L. Martin, P. J. Hay, J. E. Peralta, G. E. Scuseria, *J. Chem. Phys.* **2004**, *121*, 2144; b) G. A. Shamov, G. Schreckenbach, T. N. Vo, *Chem. Eur. J.* **2007**, *13*, 4932.
[39] a) C. Clavaguera-Sarrio, V. Vallet, D. Maynau, C. J. Marsden, *J. Chem. Phys.* **2004**, *121*, 5312; b) L. Gagliardi, M. C. Heaven, J. W. Krogh, B. O. Roos, *J. Am. Chem. Soc.* **2005**, *127*, 86.
[40] W. Koch, M. C. Holthausen, *A Chemist's Guide to Density Functional Theory*, 2nd ed., Wiley-VCH, New York, **2001**.
[41] H. G. Cho, L. Andrews, C. Marsden, *Inorg. Chem.* **2005**, *44*, 7634.
[42] P. J. Hay, *Faraday Discuss.* **2003**, *124*, 69.
[43] Th + $S_2$: B. Liang, L. Andrews, *J. Phys. Chem. A* **2002**, *106*, 4038.
[44] U + $S_2$: B. Liang, L. Andrews, N. Ismail, C. Marsden, *Inorg. Chem.* **2002**, *41*, 2811.
[45] Th + $CH_3X$: J. T. Lyon, L. Andrews, *Inorg. Chem.* **2005**, *44*, 8610.
[46] U + $CH_3X$: J. T. Lyon, L. Andrews, *Inorg. Chem.* **2006**, *45*, 1847.

Received: May 7, 2008
Published online: September 2, 2008

  